

# LARGE-EDDY SIMULATIONS OF STRATOCUMULUS TO CUMULUS TRANSITION

Marcin J. Kurowski<sup>1</sup> \*, Dorota Jarecka<sup>2</sup>, Hanna Pawlowska<sup>2</sup> and Wojciech W. Grabowski<sup>3</sup>

<sup>1</sup>Institute of Meteorology and Water Management - National Research Institute, Warsaw, Poland

<sup>2</sup>Institute of Geophysics, Faculty of Physics, University of Warsaw, Poland

<sup>3</sup>National Center for Atmospheric Research, Boulder, Colorado, USA

## 1. INTRODUCTION

The vast fields of subtropical marine stratocumulus off the western coasts of continents are known for their persistent existence. In these regions, the large-scale subsidence associated with Hadley circulation provides favorable conditions for the formation of strong inversion, which separates moist and cool stratocumulus-topped boundary layer (STBL) from dry and warm free atmosphere above. A quasi-steady equilibrium of the STBL results from a subtle balance between subsidence and mass exchange (*i.e.* small-scale entrainment) around the inversion. A faithful representation of a brake-up of solid cloud deck and its subsequent transition to cumulus field is of a great importance to the Earth's radiative budget as the process leads to a significant change in the planetary albedo. However, the fidelity with which the contemporary mesoscale/climate atmospheric models reconstruct the transition is still insufficient. It suffers from our poor understanding of a complex nature of the processes involved as well as their multi-scale coupling. The progress is also conditioned by both temporarily and spatially limited observational data while explicit representation of all scales in the models is far beyond their capabilities.

The large-eddy simulations (LES) are one of basic tools that helps to our understanding of large-Reynolds number atmospheric flows. With an explicit representation of only the largest and most energetic scales this approach substantially reduces complexity of the problems found in atmospheric modeling. In spite of its great usefulness, the question remains to what extent this approach is consistent with the observations and what the main obstacles are in accurate LES modeling of stratocumulus to cumulus transition. These issues are partially being addressed in the EUCLIPSE project. In the project, a model inter-comparison study was designed based on ASTEX observations (Bretherton et al., 1999). University of Warsaw participates in the project with the anelastic nonhydrostatic model EULAG (see e.g.

Prusa et al., 2008). The model, a well-established research fluid flow solver, is widely used in various atmosphere-related problems ranging from small-scale turbulence to planetary flows. In this study, the focus is on modification of the solver to LES modeling of a multi-hour evolution of the Sc to Cu transition.

## 2. SETUP OF THE EXPERIMENT

The numerical experiment is based on the data collected during the ASTEX Lagrangian field campaign. The initial profiles correspond to a shallow (700 m-deep) boundary layer that includes 400 m-deep cloud layer, capped with a fairly sharp inversion (temperature jump of 5.5 K over 50 m). The sea surface temperature (SST) increases gradually over time, from 290.4 K to 294.7 K over 40 hours. The large-scale subsidence evolves as well, decreasing by a factor of five compared to the initial value. Evolution of the SST and large-scale subsidence mimics Lagrangian drift of the air column towards the equator observed during the field project.

The uniform horizontal grid length is 35 m while stretched grid is applied in the vertical. The vertical grid length decreases from 15 m near the surface to 5 m in the upper part of domain, starting to compress around the initial cloud top height. The domain size is  $4.48 \times 4.48 \times 2.4 \text{ km}^3$  (*i.e.*  $128 \times 128 \times 400 \approx 6.5 \times 10^6$  grid points), and periodic lateral boundaries are assumed. The computations last 40 hours starting at 00:00 UTC.

## 3. ADAPTATION OF THE MODEL

To develop atmospheric LES model capable in realistic simulation of diurnal cycle of precipitating STBL, a set of modules was modified or added to EULAG. The most important changes are reported in this section.

### a. Radiation

Two different radiation schemes were examined in the experiment. First, the simplified long-wave radiative cooling (Stevens et al., 2005) was implemented along with a short-wave radiation from the Dutch Atmospheric Large Eddy

---

\* Corresponding author: e-mail: mkuro@igf.fuw.edu.pl

Simulation (DALES) model (Heus et al., 2010). This approach, however, was found to be insufficient in the long-term simulations. The solutions were strongly sensitive to a set of parameters proposed in Stevens et al. (2005); it was difficult to balance both radiative cooling and large-scale subsidence above the inversion; and gradual smoothing of the temperature inversion was observed. All those effects are relatively small but errors accumulate in time. After about 10 h their contribution to the solution is noticeable. Since the analyzed case is sensitive to the radiative effects, we decided to implement full radiation scheme. The radiation schemes comes from CCM2 climate model (Hack et al., 1993). The scheme works in extended vertical domain (up to 48km) and employs a pressure coordinate system. Since the radiation is computationally expensive, radiative fluxes are calculated once every two minutes and remain unchanged until the next calculation. A more expensive time interval of one minute was also tested, but the results were only a few percent different in terms of the domain averaged liquid water path and entrainment velocity.

#### b. Large-scale subsidence

As in other models, implementation of the large-scale subsidence is based on the upstream advection scheme. Subsidence velocity results from the integration of the continuity equation applying evolving horizontal divergence. The large-scale subsidence is assumed constant above 1600 m.

#### c. Subgrid-scale mixing

The subgrid-scale turbulent transport is one of the key processes that affect the entrainment velocity and thus development of STBL. Too intense entrainment of dry and warm air from a free atmosphere leads to excessive dilution of stratocumulus and its premature decay. On the other hand, too little entrainment suppresses development of the whole layer and postpones transition from Sc to Cu. To find setup suitable for this case, two different subgrid-scale schemes (SGS) were examined, namely, Smagorinsky (1963) or Schumann (1991), the latter based on the subgrid-scale turbulent kinetic energy (TKE) closure. Although both schemes are commonly used in LES modeling, the choice of basic parameters, such as the Prandtl number ( $Pr$ ) or the turbulent mixing length ( $\Lambda$ ), is uncertain. This is because the schemes were originally developed for dry convection with the grid-box aspect ratio of one. In contrast, model grid-boxes are strongly non-uniform in the EUCLIPSE setup, boundary layer is moist, and the essential subgrid-scale processes occur within a thin stably-stratified inversion layer rather than across neutrally stratified layer below. We selected  $Pr = 1$

and  $\Lambda = \Delta z$ . The former is typical for stable stratification and the latter corresponds to the vertical gridlength.

#### d. Surface fluxes

Surface sensible and latent heat fluxes are calculated applying a prescribed value of the drag coefficient (here  $C_d = 0.0014$ ) and depend on both the flow and the sea surface conditions, namely

$$F = -C_d|U|(q - q_{surf}), \quad (1)$$

where  $F$  is the flux;  $U$  is the near-surface flow velocity;  $q$  represents either the water vapor mixing ratio (for the latent heat flux) or the temperature (for the sensible heat flux) right above sea surface; and  $q_{surf}$  denotes the surface value (the sea surface temperature or the saturated water vapor mixing ratio corresponding to the surface temperature).

#### e. Microphysics

To represent processes of drizzle formation in stratocumulus, we first examined a bulk parameterization of Kessler (1969) warm rain initiation, which is commonly used in LES modeling of convective clouds. The scheme assumes linear dependence of autoconversion rate on the excess of cloud water ( $q_c$ ) over a given threshold ( $q_{tr}$ ). Since the value of a threshold is rather arbitrary, a set of different  $q_{tr}$  was tested. A strong sensitivity of the results to  $q_{tr}$  was found, especially for extreme values of the domain averaged liquid water path (LWP). For instance, the maximum LWP of 160 g/m<sup>2</sup> was simulated for  $q_{tr} = 0.68$  g/kg, whereas 170 g/m<sup>2</sup> for  $q_{tr} = 0.70$  g/kg. This is because Sc is almost uniform and the cloud water mixing ratio closely follows adiabatic profile within each column, with  $q_c$  increasing almost linearly with altitude. Therefore, arbitrary definition of  $q_{tr}$  imposes also arbitrary level above which drizzle formation is allowed.

To improve representation of the autoconversion, two other parameterizations, namely, Berry and Reinhardt (1974) and Khairoutdinov and Kogan (2000; hereafter KK2000), were examined. They both operate on mean volume radius of the cloud water rather than explicit value of the cloud water mixing ratio. The former scheme is often applied in simulations of convective clouds, whereas the latter was proposed for LES models of STBLs.

The use of Berry and Reinhardt (1974) scheme resulted in a very intense drizzle initiation along with a rapid fallout of precipitation. For instance, reduction of the initial LWP by more than 30% during the first four hours was simulated. Furthermore, sensitivity of the results to the parameters describing cloud droplet spectrum (*e.g.*,

the spectral dispersion) was fairly weak and it could not reverse the strong negative LWP trend.

The final microphysical setup is based on KK2000 drizzle parameterization. Because the KK2000 is designed for a double-moment bulk microphysics scheme (i.e., predicting both the concentrations and mixing ratios of cloud droplets and drizzle drops), we assumed a constant droplet concentration (100 per cc) for the autoconversion and accretion, and a constant sedimentation velocity of 0.72 m/s for drizzle sedimentation. Further improvements applying the double-moment scheme are being considered.

### 3. RESULTS OF THE SIMULATIONS

A large number of simulations, including many sensitivity studies, was performed to examine and adjust each element of the model. The results of that part were shortly described in previous section. Here, we present and discuss the solution provided by EULAG for the final setup.

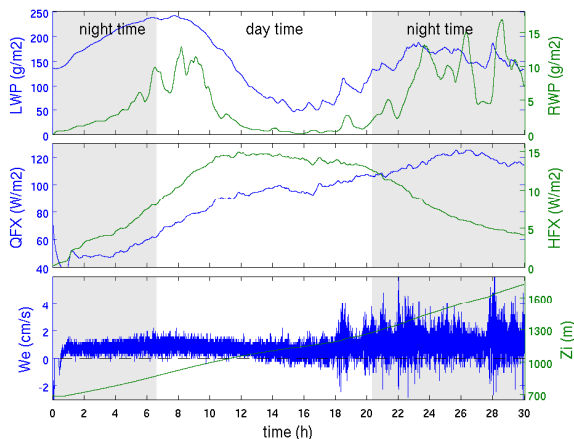


Figure 1: Time evolution of the domain averaged scalars: LWP, RWP, QFX, HFX, We and Zi (see text for details).

A typical development of STBL is shown in Fig. 1. The figure shows evolution of the following domain averaged scalars: the liquid water path (LWP), rain water path (RWP), surface sensible heat flux (HFX), surface latent heat flux (QFX), inversion height ( $Z_i$ ), and entrainment velocity ( $We$ ). During the night, the long-wave radiative cooling combined with relatively large surface latent heat flux ( $45\text{--}50\text{ W/m}^2$ ) leads to a gradual increase of LWP. As a result, RWP increases to more than  $10\text{ g/m}^2$  shortly after a sunrise (around 06:40). During the day, solar radiation reverses that trend because the cloud layer is heated throughout its entire depth. After 16 hours, LWP and RWP both reach their minima of  $50\text{ g/m}^2$  and  $0.5\text{ g/m}^2$ , respectively. With weakening solar heating, LWP and RWP begin to increase again. Entrainment velocity is positively

correlated with changes of LWP because a slower growth of the boundary layer depth is observed for a thinner cloud. During the second night, the cloud layer becomes less uniform, and the amplitude of  $We$  fluctuations as well as LWP and RWP all increase. After 30hrs, the STBL depth is already twice as large as the initial one.

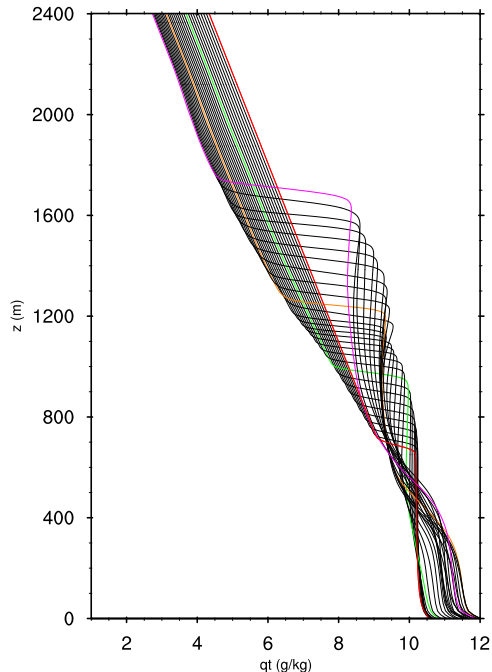


Figure 2: Hourly averaged mean profiles of the total water mixing ratio for 30 h of simulation. Each profile represents one hour (1 h - red, 10 h - green, 20 h - orange, 30 h - magenta).

To better understand the evolution of STBL, a set of hourly averaged vertical profiles is shown in Figs. 2-6. The profiles of  $q_t$  (Fig. 2) and  $\theta_l$  (Fig. 3) document drying and warming of the free atmosphere by the large-scale subsidence. As the subsidence weakens with time, the radiative cooling begins to prevail over the subsidence after about 20 hours and the free-atmospheric temperature tendency turns to negative. The initially well-mixed STBL is affected by the buoyancy production at the layer top (negative, due to radiative cooling) and the layer bottom (positive, due to surface fluxes). These are responsible for the generation of downdrafts and updrafts, which in turn enhance turbulence and vertical mixing across the STBL. Although STBL remains well mixed in  $\theta_l$ , continuous supply of water vapor from the ocean, as well as precipitation and drying of the STBL top, all lead to the decoupling observed in  $q_t$  and also  $\langle w'w' \rangle$  (Fig. 4). The difference between mean  $q_t$  at the height of 200 m and 1200 m after 30 h is more than  $2\text{ g/kg}$  (around 20%).

Fig. 5 shows evolution of the cloud water ( $q_c$ ) profiles. For Sc, the cloud remains close

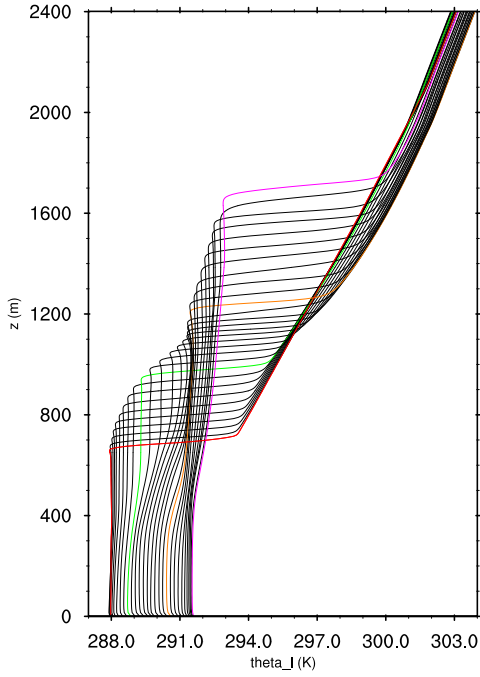


Figure 3: Hourly averaged mean profiles of the liquid water potential temperature for 30 h of simulation. Each profile represents one hour (1 h - red, 10 h - green, 20 h - orange, 30 h - magenta).

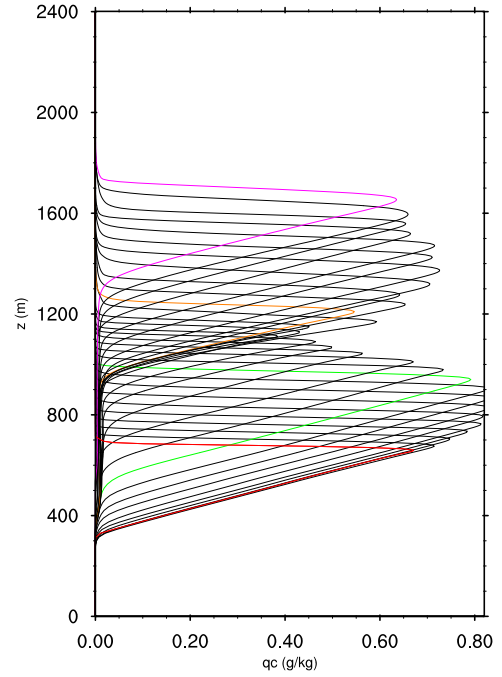


Figure 5: Hourly averaged mean profiles of the cloud water mixing ratio for 30 h of simulation. Each profile represents one hour (1 h - red, 10 h - green, 20 h - orange, 30 h - magenta).

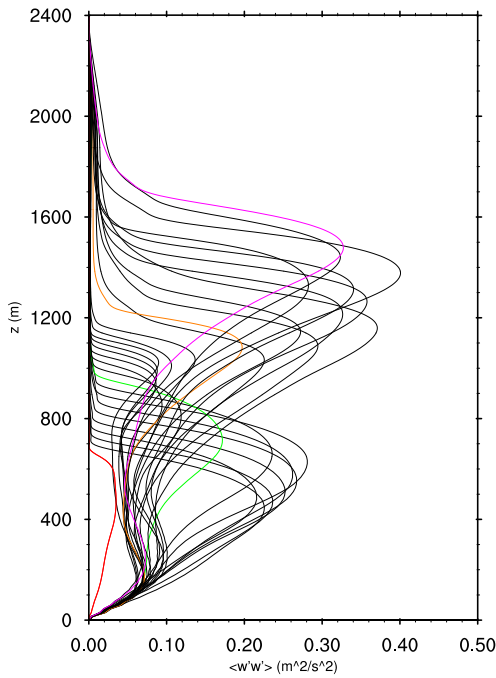


Figure 4: Hourly averaged profiles of the  $\langle w'w' \rangle$  for 30 h of simulation. Each profile represents one hour (1 h - red, 10 h - green, 20 h - orange, 30 h - magenta).

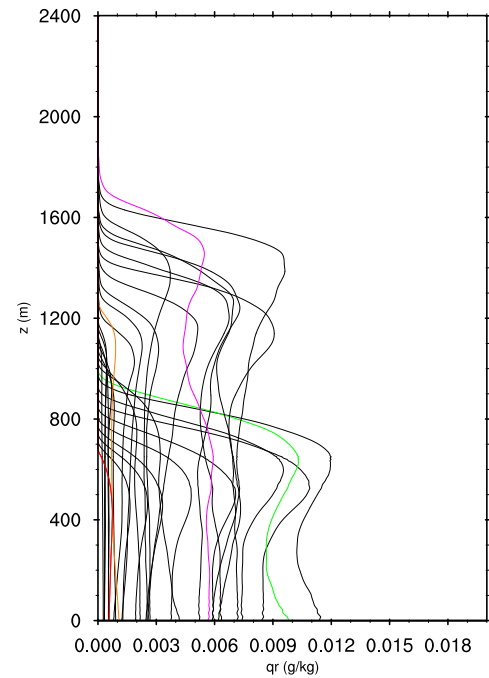


Figure 6: Hourly averaged mean profiles of the rain water mixing ratio for 30 h of simulation (1 h - red, 10 h - green, 20 h - orange, 30 h - magenta).

to adiabatic at all times due to efficient mixing within the STBL. The mean cloud top height follows the evolution of inversion level, but the cloud base rises only about 250 m after 30 h. The cloud

layer below stratocumulus, with mean  $q_c$  values of just a few hundredths of g/kg or less, represents a field of scattered shallow convective clouds that forms during the course of the simulation. The

sub-layer of broken Cu thickens in time and at the end represents about 50% of the cloud field depth.

Evolution of the drizzle mixing ratio profiles is shown in Fig. 6. The maximum of the drizzle water is observed at 11 h (0.012 g/kg). Although the autoconversion is less efficient at later hours, the second night is characterized by similar RWP values as during the first night time. This is because precipitating water falls out from a much larger altitude as the top of STBL systematically increases in time.

#### 4. SUMMARY AND CONCLUSIONS

In this study, modifications of the anelastic nonhydrostatic model EULAG to LES setup designed for simulating Sc to Cu transition was presented along with many-hour simulation results. The STBL evolution is characterized by a continuous increase of its depth and a gradual decoupling of its internal structure. A sub-layer of broken Cu develops beneath close-to-solid St. According to the results of sensitivity tests, radiation, microphysics and subgrid-scale transport at the cloud top all play vital role in the simulation, and their interactions strongly affect evolution of the boundary layer. When simulating cloud-top radiative cooling, a full radiation scheme has demonstrated its clear advantage over a simplified approach, especially for multi-day simulations. The microphysical schemes, commonly used in Cu modeling, turned out to produce too much precipitation when used for the representation of drizzle. The most realistic results were obtained for Sc-oriented microphysics, full radiation scheme, and relatively small mixing length used in subgrid-scale turbulent transport scheme. Results of subsequent studies will be presented at the conference.

#### 5. REFERENCES

- Bretherton, C. S., S. K. Krueger, M. C. Wyant, P. Bechtold, E. van Meijgaard, B. Stevens, and J. Teixeira, 1999: A GCS boundary-layer cloud model intercomparison study for the first ASTEX Lagrangian experiment. *Bound.-Lay. Meteor.*, **93**, 341-380.
- Berry, E. X., and R. L. Reindhart, 1974: An analysis of cloud drop growth by collection. Part II. Single initial distributions. *J. Atmos. Sci.*, **31**, 1825-1831.
- Hack, J. J., B. A. Boville, B. P. Briegleb, J. T. Kiehl, P. J. Rasch, D. L. Williamson, 1993: Description of the NCAR Community Climate Model (CCM2), *NCAR Technical Note*, NCAR/TN-382+STR
- Heus, T., C. C. van Heerwaarden, H. J. J. Jonker, A. Pier Siebesma, S. Axelsen, K. van den Dries, O. Geoffroy, A. F. Moene, D. Pino, S. R. de Roode, and J. Vila-Guerau de Arellano, 2010: Formulation of the Dutch Atmospheric Large-Eddy Simulation (DALES) and overview of its applications. *Geosci. Model Dev.*, **3**, 415-444.
- Kessler, E., 1969: *On the Distribution and Continuity of Water Substance in Atmospheric Circulations*. *Meteor. Monogr.*, No. 32, Amer. Meteor. Soc., 84 pp.
- Khairoutdinov, M., and Y. Kogan, 2000: A new cloud physics parameterization in a large-eddy simulation model of marine stratocumulus. *Mon. Wea. Rev.*, **128**, 229-243.
- Prusa, J. M., P. K. Smolarkiewicz, and A. A. Wyszogrodzki, 2008: Eulag, a computational model for multiscale flows. *Comp. and Fluids*, **37**, 1193-1207.
- Smagorinsky, J., 1963: General circulation experiments with the primitive equations. *Mon. Wea. Rev.*, **91**, 99-164.
- Schumann, U., 1991: Subgrid length-scales for large-eddy simulation of stratified turbulence. *Theor. Comput. Fluid Dyn.*, **2**, 279-290.
- Stevens, B., and Co-authors, 2005: Evaluation of large-eddy simulation via observations of nocturnal marine stratocumulus. *Mon. Wea. Rev.*, **133**, 1443-1462.

#### Acknowledgements

The authors would like to express sincere gratitude to Swiss National Computing Center and National Center for Atmospheric Research for providing computational resources. The National Center for Atmospheric Research is operated by the University Corporation for Atmospheric Research under sponsorship of the National Science Foundation. The technical support from Johan van der Dussen is also gratefully acknowledged.

This work has been funded by the European Commission 7th Framework programme project EUCLIPSE, contract no. 244067.